ISSN 1070-4272, Russian Journal of Applied Chemistry © Pleiades Publishing, Ltd., 2024.

SORPTION
AND ION EXCHANGE PROCESSES

Carbon Dioxide Adsorption Study on Rice Husk Activated Carbons by Artificial Neural Network (ANN)

Kishor Palle[a],*, Sambhani Naga Gayatri[a], Ramesh Kola[b], Ch Sandhya Rani[c], P. Ramesh Babu[d], L. Vijayalakshmi[e],, Seong Jin Kwon[e], and Md. Mustaq Ali[f]**

[a] *Chemistry Division, Department of H&S, CVR College of Engineering, Ibrahimpatnam, Hyderabad, Telangana State, 501510 India*
[b] *Department of Chemistry, Chaitanya Bharathi Institute of Technology (A), Gandipet, Hyderabad, Telangana, India*
[c] *Department of Computer Science & Engineering, VNR Vignana Jyothi Institute of Engineering and Technology, Hyderabad, Telangana, India*
[d] *Department of Physics, Gokaraju Rangaraju Institute of Engineering & Technology, Hyderabad, Telangana, India*
[e] *Department of Automotive Engineering, Yeungnam University, Gyeongsan-si, Republic of Korea*
[f] *Department of Mathematics (H&S), Malla Reddy Engineering College (Autonomous), Main Campus, Secunderabad, Telangana, India*
**e-mail: drkishorepalle@gmail.com*
***e-mail: lvl.phy@gmail.com*

Received January 21, 2024; revised February 28, 2024; accepted February 28, 2024

Abstract—In this study, the effects of artificial neural networks on CO_2 adsorption on several types of rice husk activated carbon samples are investigated. Using conventional approach, the eight activated carbon samples are examined for carbon dioxide adsorption at 298 K and up to 1 bar pressure. The influence of altered training/validating ratios, various data initiation points, various training algorithms and number of neurons necessary for an artificial neural network model were investigated using ANN modelling. The work can give useful information on the effects of each of the investigated factors, which are crucial in ANN modelling and training techniques. The results may be used to create an optimum activated carbon, improved applications of gas and oil purification that plan to use artificial intelligence modelling in their evaluations.

Keywords: rice husk, activated carbons, CO_2 adsorption, artificial neural network

DOI: 10.1134/S1070427224020010

INTRODUCTION

A prominent source of biomass in South Asia, along with India and China, is rice husk. There is a high utilization value for rice husk as ash when compared to other farming bio-waste materials, mostly in the form of silica, and a low utilization value as husk. Organic matter from rice husks has been used for energy and has high value-added potential for other applications as well. A total of more than 650 million tons of rice are produced every year around the world, making it the third most significant cereal crop [1]. A major by-product of rice processing mills is rice husk, a protective layer for rice grain [2, 3]. Rice husk contain, %: cellulose 32.24, hemicelluloses 21.34, lignin 21.44, water 8.11, extractives 1.82, and mineral ash 15.05, with a high percentage of 94.5–96.34% silica in its mineral ash [4, 5]. Figure 1 illustrates the components of rice husk.

Rice husks are notable for their low level of utilization when compared to scrap of wood and maize straw, but high level of utilization when compared to their ash [6, 7]. The silica in rice husk makes it an ideal silicon source. It is commonly used to synthesize cement, filter aids, silicides, and other materials [8, 9]. The silica in RHA is predominantly composed of amorphous cristobalite, which is predominant in the mineral [10].

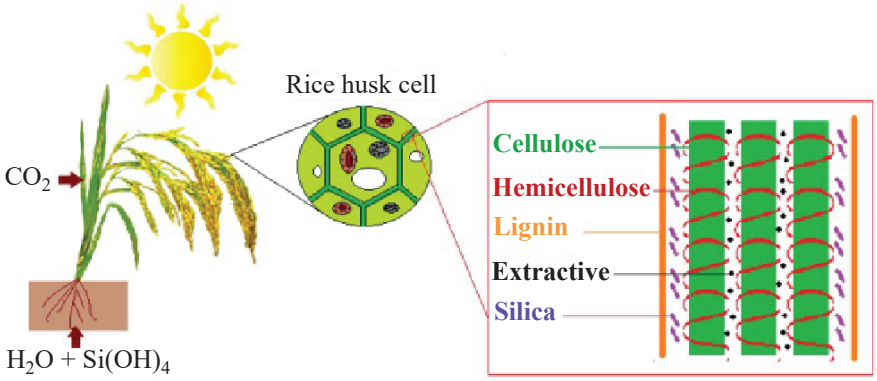

Fig. 1. Illustration of components of rice husk.

Reinforcement of cement can also be accomplished with rice husks [11]. In addition to serving as a catalyst carrier [12] and low-cost adsorbent [13], rice husk has a very good porous nature [14].

After petroleum and coal, natural gas is the world's third most used energy source. Presently, gases have a significant impact on the energy sector [15]. Gases are employed in a variety of applications, including industry and energy distribution. In terms of carbon emissions, however, gas pollution is half that of petroleum [16]. As a result, natural gas plays a significant role as a fuel that's environmentally friendly. Unconventional reservoirs are ultra-tight earth basements that can generate natural gas. Because CO_2 offers configurable features in terms of dissolving capacity and viscosity under varied working settings, it is considered one of the most often used approaches.

The ANN has has been getting a lot of attention lately due to its precision in predicting intricate physical and chemical processes. The ANN model necessitates greater focus on testing, validation, and data points for training. Additionally, the number of neurons needed to train an ANN model cannot be computed quantitatively since mathematical computation is not available. Equally significant is the ANN algorithm in terms of model accuracy [17]. In light of the previous explanation regarding natural gases, this study investigated the adsorption of carbon dioxide on activated carbon samples. A study was conducted to demonstrate the use of neural network modeling and artificial intelligence for the adsorption capacity prediction of activated carbon samples. A study based on artificial intelligence may be useful for adsorption and production of CO_2 from unconventional gases and activated carbon preparations.

In order to comprehend the behaviour of activated carbons, sorption studies is often carried out at high pressure and temperature conditions in reservoir . Studying supercritical CO_2 sorption and simulating field operating circumstances are the objectives of high adsorption research [18]. In most practical research, equilibrium isotherm models are used to observe adsorption analysis; however, these models are not always the most precise. Most isotherm models have measurement issues with regard to porosity, pressure, and even temperature. Consequently, there is a clear need for more precise and comprehensive application modelling in order to better understand the relationship between sorption capacity and selectivity as well as the porous media under investigation, such as activated carbon.

The buoyancy effect commonly affects the analysis of CO_2 adsorption at working pressures of up to 200 bar, and this needs to be adjusted by the usage of equation for different states. Consequently, there is a notable increase in the uncertainty of the measurement [19]. Adjustments to the sample weight or isothermal pressure conditions are frequently used to determine adsorption capacity. These parameters and variables are associated to alter the circumstances that predominate. However, no study has combined field operational features in a thin porous medium with the distribution of pores for more creative applications and assessments of gas recovery.

Gopalan et al. investigated the studies of gas adsorption using AIML techniques by many researchers based on ML modelling of hydrogen adsorption in past research [20]. For this adsorption in nanoporous materials modeling based on Gaussian process regression (GPR) was applied. The number of hydrogen (n_1) was

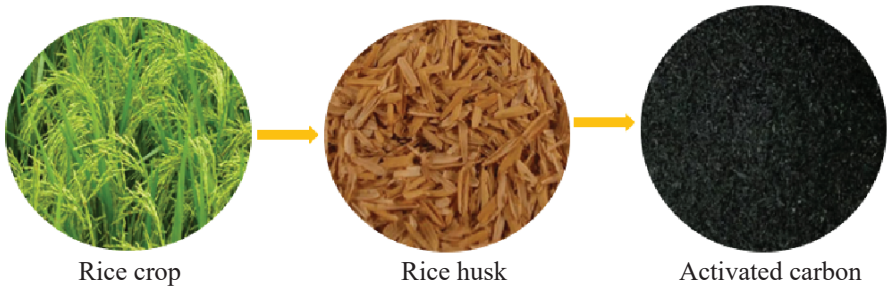

Fig. 2. Digital images of rice crop, rice husk and activated carbon.

calculated using GPR as a void fraction (φ), function of adsorption pressure and the greatest pit diameter. The accuracy of the generated machine learning model was comparable to that of Machine learning [21–24], large standard Monte–Carlo simulations [25] is employed in the adsorption studies isotherm modelling (S_{BET}) [26, 27] created an artificial neural network model to analyse the isotherms with surface area.

To predict adsorption created ANN model has been trained with the least amount of error and the highest level of accuracy. The constructed model was tested on 1000 data points gathered by a literature review and an experimental investigation, and it performed well. According to the findings, mesopores play an important role in limiting CO_2 absorption, whereas for gas adsorption micropores are required [28]. One more significant finding of the study was the effect of solid absorbents on gas desorption on textural parameters, as well as the sensitivity of specific parameters that may be evaluated. Wang et al. created a convolution neural networks model to predict carbon dioxide and nitrogen adsorption at 77k with varied porosity ranging from 3–7 nm of mesosphere to less than 2 nm of micropores to examine carbon dioxide and nitrogen adsorption by the influence of pore size distribution [29]. According to the established model, optimal adsorption exhibited by microporous surfaces [30–32].

MATERIALS AND METHODS

For this investigation, rice husk was collected from a rice mill near Telaprolu in Vijayawada, India. It was thoroughly cleansed with distilled water to remove any dirt or dust that had adhered, and it was then dried at 110°C overnight. For four hours, rice husks were calcined at various temperatures and in various atmospheres. The gas flow was kept at 40 mL per minute, and the temperature was set at 10°C per min [33]. At different activation temperatures such as 400, 500, 600, and 700, four activated carbon samples from rice husk were prepared. An atmosphere of nitrogen-carbon dioxide was used for the process (18 dm^3/h nitrogen flow, 5 dm^3/h carbon dioxide flow). In all the experiments, time, N_2-CO_2 flow rate, and furnace heating rate remained the same. We treated the activated carbon with 1 M HCl solution for 20 h and left it behind. As a next step, deionized water was used to rinse the carbons until chloride ions were completely removed. In the following step, samples were dried for 16 h at 110°C. As a result, RHAC-400, RHAC-500, RHAC-600, and RHAC-700 were chosen for the activation process. RHAC stands for rice husk activated carbon. Digital images of rice crop, rice husk, and its activated carbon were shown in Fig. 2 [34].

BET method was used on a BELSORB II Instrument, Japan, to estimate the surface area of activated carbon samples. To remove the contaminants from samples, the adsorption measurements were preceded by heating at temperature of 250°C for 12 h with the heating rate of 1°/min under the reduced pressure.

The porous structure parameters have been derived from the N_2 sorption isotherms.

Surface area (S_{BET}) estimated on the basis of the BET equation with the partial pressure in the range of p/p_0 = 0.05–0.2. This range was pointed independently for each material so that a linearity of function (1) were fulfilled:

$$f\left(\frac{p}{p_0}\right)=\frac{1}{W\left(\frac{p}{p_0}-1\right)}, \quad (1)$$

where W is the mass of gas adsorbed at a relative pressure p/p_0, p is the nitrogen pressure, p_0 is equal to 1.01 bar;

Total pore volume (V_p, N_2) calculated from the maximum adsorption of nitrogen vapor for p/p_0 = 0.99;

Fig. 3. Manual setup for CO_2 adsorption studies

Pores in a range of micropores (V_{micro}, N_2) and mesopores were evaluated using N_2 analysis at –196°C temperature by the density functional theory (DFT) method.

In this work, high purity CO_2 and He gases with a purity of 99.995% were used for adsorption and pre-measurement assortments. The gas was supplied by a local gas company Lakshmi agencies. The primary physicochemical parameters that could impact the adsorption process were investigated using sample characteristics. The CO_2 adsorption capacity of activated carbon samples was measured using thermal conducting detector-gas chromatography (TCD-GC) and a pneumatically controlled sample injector at 289 K and up to 1 bar [25]. Manual setup of CO_2 adsorption study represent in Fig. 3. A total of 20 evenly spaced segments were used to quantify adsorption and desorption at the same time. Training-to-validating ratios, initiation data points and alternating training algorithms were used in the ANN modelling [21].

Samples were crushed, screened, and homogenized in order to achieve particle sizes of 0.5–1 mm. In the present study, X-ray powder diffraction (XRD) patterns of the catalysts were recorded by a Rigaku Miniflex (Rigaku Corporation, Japan) X-ray diffractometer using Ni filtered Cu K_α radiation (λ = 1.5418 Å) with a scan speed of 2° min^{-1} and a scan range of 10-80° at 30 kV and 15 mA. The BET surface area of the catalysts was measured at –196°C using a commercial multi-point QUADRASORB SI (Quantachrome Instruments, USA) by N_2 physisorption.

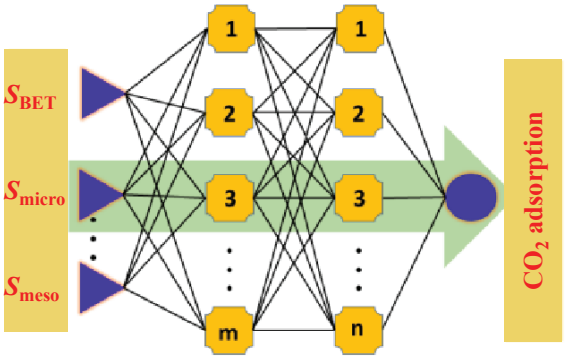

Fig. 4. Construction of ANN (artificial neural network)

Artificial Neural Network Method

Based on research by North and colleagues, V_{micro} and V_{meso} levels had an impact on the amount of CO_2 that could be absorbed [35]. In accordance with additional study, porous carbons' large surface areas and small micropores promote more CO_2 adsorption. In order to better comprehend the functions of S_{BET}, V_{micro}, and V_{meso}, we selected input layer variables as neurons, which were subsequently sent to hidden layers and output layers. A typical neural network (NN) construction is shown in Fig. 4. When a neural network contains more than one hidden layer, it is referred to as a deep neural network (DNN). Weights are represented by lines connecting two nodes, which simulate input-output relationships [34].

RESULTS AND DISCUSSION

The textural properties of all the activated carbon samples were compiled in Table 1.

As a result of the isotherms, microporous samples exhibited high N_2 adsorption at low relative pressures. All carbon samples exhibited a notable increase in nitro-

Table 1. Textural parameters for activated carbons, derived from N_2 adsorption isotherms at –196 °C.

Sample	S_{BET}, m^2/g	V_p, N_2, cm^3/g	V_{micro}, N_2, cm^3/g
RHAC-400	248	0.63	0.39
RHAC-500	576	0.72	0.52
RHAC-600	1074	1.42	0.45
RHAC-700	124	0.35	0.06

gen adsorption at a temperature of –196°C as the activation temperature during thermal treatment increased. However, there was one exception to this trend. The carbon sample activated at the highest temperature (700°C) achieved the lowest nitrogen capacity.

The results of undermentioned adsorption-desorption isotherms of N_2 on the examined activated carbons are shown in Fig. 5.

Equation 2 is used to determine adsorption capacity of the activated carbon.

$$q = \frac{m_i - m_f}{w} = \left(\frac{VM_w}{Rw}\right)\left(\frac{P_i}{Z_i T_i} - \frac{P_f}{Z_f T_f}\right), \quad (2)$$

$$Z = 1 + \frac{BP}{RT}. \quad (3)$$

An initial and final condition is indicated by the subscripts i and f. P, V, R, Z, and w stand for pressure, temperature, reactor volume, and universal gas constants for rice husk adsorption, respectively. Virial equation (Eq. 3) was used for the calculation of the compressibility factor [36]. An adsorption experiment was conducted at 0°C and 1 bar of pressure on activated carbon surfaces. The experimental CO_2 capacity at 0°C are given in Fig. 6.

The current investigation incorporated the input parameters of pressure and temperature. A process response or output variable was generated by adsorption on the CO_2 amount (AC) adsorption. By adjusting 4 to 10 number of neurons with a time step of 1, the adsorption model was created. ANN is trained utilizing the statistical parameter of mean square errors (MSE). The MSE and correlation coefficient (R^2) were calculated using Eqs. 4 and 5, respectively [37]. Table 2 represents calculated and recorded the mean squared error and R squared values.

Table 2. Calculated mean squared error and R squared values for different neurons

Hidden neurons	Mean squared error value (for test)	R squared value
4	0.0992	0.8971
5	0.0794	0.9064
6	0.1224	0.9895
7	0.0022	0.9875
8	0.0198	0.9658
9	0.1134	0.9121
10	0.2286	0.9062

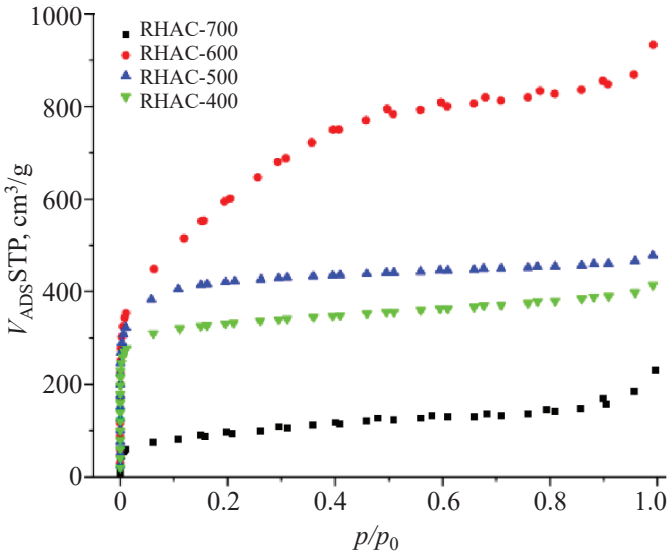

Fig. 5. The adsorption-desorption isotherms of N_2 for activated carbons.

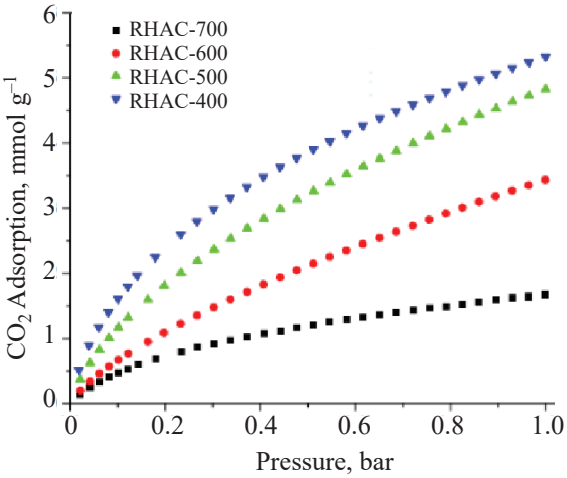

Fig. 6. CO_2 adsorption isotherms measured at 0 ◦C.

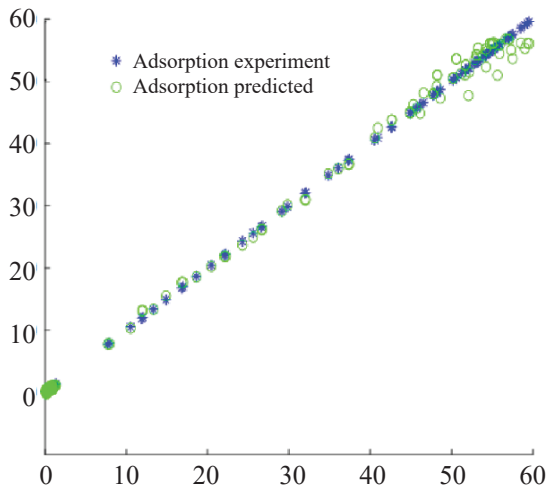

Fig. 7. Comparison of experimentally determined adsorption results and those predicted by the RNN LM algorithm.

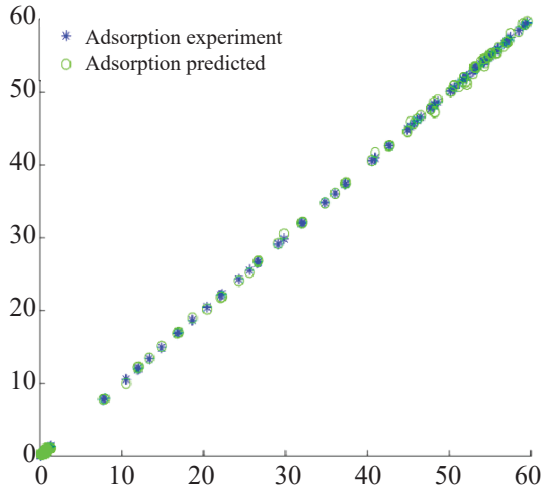

Fig. 8. Comparison of experimentally determined adsorption results and those predicted by the RNN BFGS algorithm.

$$\mathrm{MSE} = \frac{1}{N}\sum_{i=1}^{N}(Y_{\text{predocted}} - Y_{\text{real}})^2, \quad (4)$$

$$R^2 = \frac{1}{N}\sum_{i=1}^{N}\frac{(Y_{\text{predocted}} - Y_{\text{real}})^2}{(Y_{\text{predocted}} - Y_{\text{mean}})^2}. \quad (5)$$

Best R squared value and lowest mean square error value 0.0022 given by adsorption models using seven neurons. Therefore, the ANN model was generalized using this model. Figures 7 and 8 compare the adsorption results produced by the ANN model employing various algorithms using 7 neurons.

Data is normalised before being fed into a deep neural network in several research since the data came from a variety of sources. Non-normalized data points were used in this investigation because the dataset used from same experimental setup. The experiment in our lab yielded 117 CO_2 adsorption data, from this data randomly 80 were selected for neural network training using machine learning in MATLAB software. The deep learning model was tested using the remaining 27 data points.

Figure 9 shows that the predicted results are quite similar to experimental findings, with a MSE of just 2.315. In Fig. 9, the test data set is compared to experimental findings, and the results reveal that the trained model and experimental results are in excellent agreement.

The findings of this study can be used to evaluate the preliminary phases of measurements of carbon dioxide adsorption and predictions on restricted sources with great precision and accuracy utilizing various machine

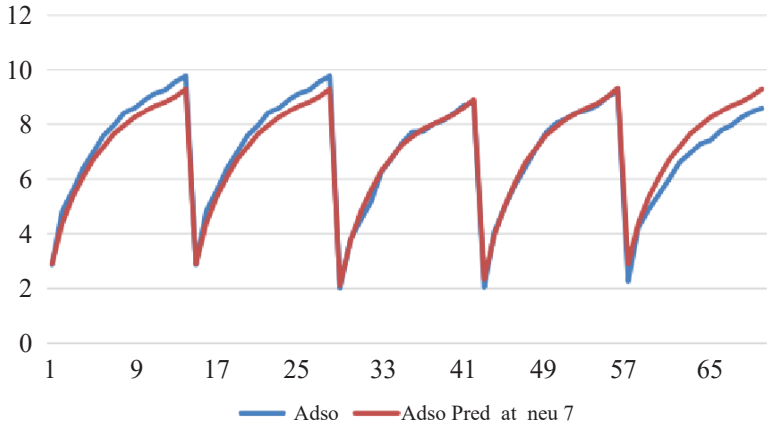

Fig. 9. comparison of predicted and experimental results of adsorption using artificial neural network model.

learning approaches based on source conditions and effects, and by the impact of processing conditions on carbon dioxide adsorption, carbon dioxide sequestration and improved recovery of oil and gas. Advanced and further research can be undertaken in order to examine the practicality of the suggested models to acquire real data from source and unconventional basins. This inquiry, on the other hand, is a first of its type and can serve as a useful benchmark for newly researched topics and expertise in crucial industries, particularly in the areas of viable productivity and energy sustainability.

CONCLUSIONS

We have generalized and optimized the mathematical model as for ANN algorithms, data initiation points and neurons. Adsorption predictions for lab experiments were accurate with this model and was used at greater pressures and temperatures to predict adsorption. Adsorption values and desorption processes can be optimized using ANN models in industry to compute adsorption values at very high temperatures and pressures.

FUNDING

This work was supported by ongoing institutional funding. No additional grants to carry out or direct this particular research were obtained.

CONFLICT OF INTEREST

The authors states that there is no conflict of interest.

REFERENCES

1. Song, X., Zhang, Y., Yan, C., Jiang, W., and Chang, C., *J. Colloid Interface Sci.,* 2013, vol. 389, p. 213.
2. Nhapi, I., Banadda, N., Murenzi, R., Sekomo, C., and Wali, U., *Open Environmental Engineering Journal,* 2011, vol. 4, p. 170.
3. Zhang, J., Fu, H., Lv, X., Tang, J., and Xu, X., *Biomass and Bioenergy,* 2011, vol. 35, 464.
4. Masoud, M.S., El-Saraf, W.M., Abdel-Halim, A.M., Ali, A.E., Mohamed, E.A. and Hasan, H.M., *Arab. J. Chem.,* 2012, vol. 9, p. S1590.
5. Wan Ngah, W. and Hanafiah, M., *Bioresour. Technol.,* 2008, vol. 99, p. 3935.
6. Wang, W, Martin, J., Zhang, N., Ma, C., Han, A., and Sun, L., *J. Nanopart. Res.,* 2011, vol. 13, p. 6981.
7. Virtanen, T., Svedström, K., Andersson, S., Tervala, L., Torkkeli, M., Knaapila, M., Kotelnikova, N., Maunu, S.L., and Serimaa, R., *Cellulose*, 2012, vol. 19, p. 219.
8. Antiohos, S.K., Papadakis, V.G., and Tsimas, S., *Cem. Concr. Res.,* 2014, vol. 20, p. 61.
9. Adam, F. and Appaturi, J.N., and Iqbal, A., *Catal. Today,* 2012, vol. 190, p. 2.
10. Chandrasekhar, S., *J. Mater. Sci.,* 2003, vol. 38, p. 3159.
11. Jaturapitakkul, C. and Roongreung, B., *ASCE J. Mater. Civ. Eng.,* 2003, vol. 15, p. 470.
12. Shinde, A.B., Shrigadi, N.B., and Samant, S.D., *J. Chem. Technol. Biotechnol.,* 2003, vol. 78, p. 1234.
13. Srivastava, V.C., Mall, I.D., and Mishra, I.M., *Chem. Eng. J.,* 2008, vol. 140, p. 136.
14. Palle, K., Yadav, G.K., Kumar, P.S., et al., *High Energy Chem.,* 2023, vol. 57, p. 83.
15. Fakher, S. and Imqam, A., *SN Appl. Sci.,* 2020, vol. 2, p. 5.
16. Rani, S., Padmanabhan, E., and Prusty, B.K., *J. Pet. Sci. Eng.,* 2019, vol. 175, p. 634.
17. Palle, K., Vunguturi, S., Gayatri, S.N., et al., *MRS Commun.,* 2022, vol. 12, p. 434.
18. Abdulkareem, F.A. and Padmanabhan, E., *Can. Chem. Eng.,* 2020, ID 23838.
19. Singh, D.K., Krishna, K.S., Harish, S., Sampath, S., and Eswaramoorthy, M., *Angew. Chemie Int. Ed.* 2016, vol. 55, p. 2032.
20. Gopalan, A., Bucior, B.J., Bobbitt, N.S., and Snurr, R.Q., *Mol. Phys.*, 2019, vol. 117, p. 3683.
21. Pardakhti, M., Moharreri, E., Wanik, D., Suib, S.L., and Srivastava, R., *ACS Comb. Sci.,* 2017, vol. 19, p. 640.
22. Subraveti, S.G., Li, Z., Prasad, V., and Rajendran, A., *Ind. Eng. Chem. Res.,* 2019, vol. 58, ID 20412.
23. Meng, M., Qiu, Z., Zhong, R., Liu, Z., Liu, Y., and Chen, P., *Chem. Eng. J.,* 2019, vol. 368, p. 847.
24. Wang, L., Liu, M., Altazhanov, A., Syzdykov, B., Yan, J., Meng, X., and Jin, K., Abstracts of Papers, *Soc. Pet. Eng.-SPE Eur. Featur. 82nd EAGE Conf. Exhib. D,* 2020.
25. Daub, C.D., Patey, G.N., Jack, D.B., and Sallabi, A.K., *J. Chem. Phys.,* 2006, vol. 124, ID 114706.
26. Dureckova, H., Krykunov, M., Aghaji, M.Z., and Woo, T.K., *J. Phys. Chem. C,* 2019, vol. 123, p. 4133.
27. Zhang, Z., Schott, J.A., Liu, M., Chen, H., Lu, X., Sumpter, B.G., Fu, J., and Dai, S., *Angew. Chemie Int. Ed.,* 2019, vol. 58, p. 259.
28. Wang, S., Zhang, Z., Dai, S., and Jiang, D., *ACS Mater. Lett.*, 2019, vol. 1, p. 558.
https://doi.org/10.1021/acsmaterialslett.9b00374

29. Wang, S., Li, Y., Dai, S., and Jiang, D., *Angew. Chemie,* 2020, vol. 132, p. 19813. https://doi.org/10.1002/ange.202005931
30. Fanourgakis, G.S., Gkagkas, K., Tylianakis, E., Klontzas, E., and Froudakis, G., *J. Phys. Chem. A,* 2019, vol. 123, p. 6080.
31. Jablonka, K.M., Ongari, D., Moosavi, S.M., and Smit, B., *Chem. Rev.,* 2020, vol. 120, p. 8066.
32. Erdem Günay, M. and Yıldırım, R., *Catal. Rev.-Sci. Eng.,* 2020, vol. 63, p. 120.
33. Palle, K., Vunguturi, S., Subba Rao, K., et al., *Chem. Pap.,* 2022, vol. 76, p. 7525.
34. Palle, K., Yadav, G.K.S., Gayatri, S.N., et al., *MRS Commun.*, 2022, vol. 12, p. 886.
35. Durá, G., Budarin, V.L., Castro-Osma, J.A., Shuttleworth, P.S., Quek, S.C.Z., Clark, J.H., and North, M., *Angew. Chem. Int. Ed.,* 2016, vol. 55, p. 9173. https://doi.org/10.1002/ange.201602226
36. Ramezanipour Penchah, H., Ghaemi, A., and Godarziani, H., *Environ. Sci. Pollut. Res.,* 2021, vol. 28, p. 55754.
37. Hemmati, A., Ghaemi, A., and Asadollahzadeh, M., *Sep. Sci. Technol.,* 2021, vol. 56, p. 2734.